Land Use/Land Cover Classification with Spectral Indices and Otsu Thresholding

Subhash Mukherjee[1], Sourav Das[1], Somnath Mukhopadhyay[1], Sunita Sarkar[1], Wangjam Niranjan Singh[1], and Ajoy Kumar Khan[2]

[1] Dept. of Computer Science & Engineering, Assam University, Silchar, Assam 788011, India
subhashmakaut@gmail.com, dassourav9957@gmail.com, som.cse@live.com, sarkarsunita2601@gmail.com, niranwang@gmail.com

[2] Dept. of Computer Science, Mizoram University, Aizawl, Mizoram 796004, India
ajoycse@gmail.com

Abstract. Accurate land use/land cover (LULC) classification is crucial for understanding environmental dynamics, monitoring natural resources, managing urban expansion, and promoting sustainable land management practices. The availability of labeled datasets is a significant obstacle to accurate land use/land cover (LULC) classification in isolated and underrepresented areas like the Barak River Basin. This study presents an unsupervised classification on Landsat 8 satellite imagery, implementing several spectral indices to overcome the insufficiency of the label data set. For vegetation identification, the Normalized Difference Vegetation Index (NDVI), Modified NDVI (MNDVI), Green NDVI (GNDVI), and Ratio Vegetation Index (RVI) were calculated. Water body detection utilized the Normalized Difference Water Index (NDWI), Modified NDWI (MNDWI), Water Ratio Index (WRI), and Automated Extraction of Water Index (AEWI). For built-up area mapping the Normalized Difference Built-up Index (NDBI), Urban Index (UI), and Built-up Index (BI) were evaluated. Amid these, it came to light that NDVI, WRI, and BI performed best for their respective categories. Otsu's thresholding technique was applied to further process these determined indices in order to classify the binary imagery of the Barak River Basin. Notwithstanding the lack of labeled training data, the thereby generated classification output was evaluated through ground truth verification and accuracy assessment, suggesting excellent performance. Utilizing the highest-performing indices, we were able to generate the label Landsat 8 imagery using an unsupervised method. In areas with inadequate information, this technique makes it possible to develop spatiotemporal datasets for long-term environmental monitoring and land management, and it determines the prerequisites for scalable LULC mapping.

Keywords: LULC · Remote sensing · Indices · Vegetation · Water · Built-up · Otsu thresholding. .

1 Introduction

Land use and land cover (LULC) classification is a cornerstone of geospatial analysis, playing a crucial role in environmental monitoring, resource management, urban planning, disaster mitigation, and policy-making. The recognition of human impacts on natural ecosystems, sustainable land management, and climate resilience plans at the regional and global levels are all made feasible by timely and accurate LULC data. Remote sensing is now a vital tool for creating LULC maps across large and varied landscapes due to the increasing availability of satellite data [14]. However, accurate land cover type discrimination is essential to extract meaningful LULC information from satellite imagery. This is a challenging endeavour because of spectral overlaps, seasonal variations, and heterogeneous landscapes [31]. Spectral indices have been established as effective measures to improve class separability by taking advantage of particular reflectance characteristics of land surface features in order to overcome this challenge. The use of specific indices, like vegetation and water indices, can accentuate the distinct spectral behaviours that vegetation, water bodies, and built-up areas display in multispectral imagery [29,15]. Yet, no single index is universally optimal across all geographical contexts or environmental conditions. Therefore, it is crucial to apply and compare several spectral indices to identify the best indicators for a given area or research goal. This method of comparison enhances classification accuracy and ensures methodological robustness, particularly in regions with complex land cover dynamics [21].

Notwithstanding these developments, a major obstacle still exists: the dearth of high-quality, easily accessible, and labelled geospatial datasets, particularly in areas with limited data and ecological sensitivity [7,31]. This problem is best illustrated by the Barak River Basin in northeastern India. Known for its rich biodiversity, intricate hydrological networks, and critical socio-economic value, the basin remains understudied in terms of fine-resolution LULC mapping [20]. The use of supervised machine learning techniques, which otherwise rule the field of remote sensing-based classification, is hampered by the lack of labelled training data [14].

This study adopts an unsupervised classification framework that incorporates several spectral indices obtained from Landsat 8 Operational Land Imager (OLI) imagery to overcome this limitation [21]. For vegetation identification, the Normalized Difference Vegetation Index (NDVI), Modified NDVI (MNDVI), Green NDVI (GNDVI), and Ratio Vegetation Index (RVI) were calculated [29]. Water body detection utilized the Normalized Difference Water Index (NDWI), Modified NDWI (MNDWI), Water Ratio Index (WRI), and Automated Extraction of Water Index (AEWI) [15]. For built-up area mapping the Normalized Difference Built-up Index (NDBI), Urban Index (UI), and Built-up Index (BI) were evaluated. These indices are systematically compared to identify the most responsive and discriminative features for the Barak River Basin.

Otsu's thresholding technique is used to enhance the delineation of land cover boundaries [17]. In the absence of valid labels, this widely recognized histogram-based image segmentation method calculates the optimal threshold values to

maximize inter-class variance, enabling a completely automated and statistically sound classification. An effective and replicable method for unsupervised LULC mapping is achieved by the combination of threshold-based segmentation and index-based clustering.

Using field surveys and high-resolution ancillary datasets to evaluate classification accuracy, validation is carried out through selective ground truthing [4,10]. This validation demonstrates our hybrid methodology's adaptability for use in other underrepresented or data-constrained regions and validates its dependability. Ultimately, an innovative and scalable geospatial framework for LULC classification in the Barak River Basin is presented in this study. By resolving the issues related to labeled data scarcity and improving classification through multi-index comparison, the proposed method helps to make better decisions in regional planning, environmental preservation, and disaster preparedness. Additionally, it highlights the critical need for adaptable techniques that can work well in situations with limited data, a recurring problem in remote sensing, especially in most of the developing world [31].

The rest of the paper is organized as follows. Section 2 presents related work in the field followed by Section 3 where data description is discussed, and section 4 presents the proposed methodology of the paper. Then the results and discussion are given in section 5. Finally, we conclude this study in section 6.

2 Related Work

The Barak River is flowing parallel to the River Brahmaputra in northeast India. Its climatic scenario is quite different from that of the Brahmaputra River basin. The basin receives mostly orographic and cyclonic precipitation with about 300 cm of average annual rainfall. With an area of 41,000 km^2, the Barak River basin is considered as one of the large basins in India. Urbanization and various infrastructural activities are going on since the last couple of decades [24,5,23]. As stated by Census of India 2011, the population growth rate is 17.93% in the Barak valley [3]. The basin area is under development and on the verge of urbanization [24,5,6]. There is almost nil industrial growth in this area, although some agricultural development can be seen [22]. This study relates to the prestage of the adverse effect of urbanization. Rich in biodiversity and agricultural productivity, the Barak Valley is currently facing increased anthropogenic pressures such as urban expansion and deforestation, leading to substantial changes in land use/land cover (LULC) dynamics [28].

Remote sensing-based spectral indices are instrumental for monitoring vegetation health, water bodies, built-up areas, and soil exposure. The Normalized Difference Vegetation Index (NDVI) is widely used to evaluate vegetation density, while the Soil-Adjusted Vegetation Index (SAVI) proposed by [9] is particularly beneficial in arid and sparsely vegetated areas. NDWI (Normalized Difference Water Index) and its enhanced version MNDWI are effective for water feature detection [15,32]. In the paper [32] they modified the NDWI by replacing the NIR band with the mid-infrared band, significantly improving water

feature extraction in urban contexts. Similarly, [25] demonstrated that integrating MNDWI with Digital Elevation Model (DEM) and groundwater data yielded a classification accuracy of 96.9% in Punjab. The paper [16] comparing three indices NDVI,NDWI and NDBI reported a strong negative correlation between NDVI/NDWI and land surface temperature (LST), and a positive correlation with NDBI, achieving an R^2 of 0.699 when using all three indices. Comparable results were observed in Bangladesh by [8], where NDVI showed a stronger correlation with forest cover changes than SAVI. A study investigated seasonal variations of NDVI, NDBI, and NDWI using LISS-III data, highlighting the temporal sensitivity of these indices [18,19].The study conducted in the paper [33] monitored urban growth from 1991 to 2019 using NDVI and NDBI, revealing significant vegetation loss and urban expansion. For built-up area detection, indices such as NDBI [34], UI, and MNDBI have proven effective. [2] developed a new spectral index for detecting built-up areas using Landsat-8 imagery, outperforming traditional indices in both accuracy and kappa values. Reviews by [12,11] comprehensively compared built-up area indices, addressing their respective limitations. Computing vegeation, water and bulit-up the paper [1] applied seasonal thresholds using NDVI, NDWI, MNDWI, and NDBI to classify LULC types, achieving 90.2% overall accuracy and a kappa coefficient of 0.84. Thresholding techniques such as Otsu's method [26] is widely used for binary classification, minimizing intra-class variance to identify optimal thresholds. [27] demonstrated the advantage of multi-Otsu thresholding in segmenting Acute Myeloid Leukemia (AML) images, achieving 83.81% accuracy with Naïve Bayes—surpassing the static Otsu method's 75.35%. Studies that incorporate multi-Otsu thresholding for LULC classification have shown improved delineation of vegetation, built-up areas, and water bodies in heterogeneous landscapes. However, these methods often require preprocessing for best performance. Accuracy assessment is fundamental to evaluating remote sensing classifications. The Cohen's Kappa coefficient, commonly used alongside overall accuracy, provides a robust measure by accounting for chance agreement. In the paper [2], high kappa values validated the effectiveness of the newly proposed index.

After studying the recent literature, we find that there are multiple spectral indices available for LULC classification, but which indices give the best result need a comparison. So, we have applied multiple indices for LULC classes like vegetation, water bodies, and built-up areas and computed the best threshold to classify into binary class. Using the best binary class, we get the unsupervised label data set for our study area.

A comparative analysis of the releated recent work on LULC classification using spectral indices is demonstrated in the Table 1. The table summarizes the methods, indices used, and reported accuracy metrics. It highlights how the proposed unsupervised method achieves superior Kappa agreement across key land cover classes while operating without labelled data.

Table 1. Comparative Analysis of Relevant Works in LULC Classification Using Spectral Indices and Thresholding

Study (Ref)	**Indices Used**	**Method Type**	**Key Findings**	**Limitations**
Bencherif et al. [1]	NDVI, NDWI, MNDWI, NDBI	Supervised (Seasonal Thresholds)	Achieved high kappa (0.84) for LULC classification	Requires labeled data and seasonal tuning
Bouzekri et al. [2]	New Built-up Index	Supervised	Developed improved built-up index (accuracy - 92.66%) better than NDBI	Limited to built-up areas, lacks general applicability
Morsy & Hadi [16]	NDVI, NDWI, NDBI	Statistical (Correlation with LST)	Demonstrated $R^2 = 0.699$ linking LULC to temperature	Not focused on classification accuracy
Singh et al. [25]	MNDWI + DEM + Groundwater	Supervised Fusion-based	Achieved 96.9% accuracy for water classification	Focused only on water; uses ancillary data
Sun et al. [26]	Otsu + Random Forest	Hybrid (Thresholding + ML)	Improved segmentation in seasonal and snowy areas	Requires training data; computationally intensive
Xu [32]	MNDWI	Thresholding	Improved water delineation in urban areas	Applied only to water class
Suryani et al. [27]	Multi-Otsu	Unsupervised (Image Segmentation)	Multi-Otsu improved classification (83.81%) vs. Otsu (75.35%)	Study focused on medical images, not remote sensing
Proposed Work	NDVI, MNDVI, GNDVI, RVI, NDWI, MNDWI, AWEI, WRI, NDBI, UI, BI	**Unsupervised + Otsu Thresholding**	**High kappa scores: NDVI (0.93), WRI (0.83), BI (0.81); general-purpose LULC mapping**	**May require empirical validation in different terrains**

3 Data Description

In this section we have discussed the process of data collection methods and selection of the desired area for the study. The Landsat Series has provided the longest temporal coverage, spanning over 52 years since 1972. Therefore, we utilized **Landsat 8** data accessed from the United States Geological Survey (USGS) EarthExplorer platform [30]. The data was acquired by Landsat 8 on **25-February-2025 at 04:18:20.7102020Z**, ensuring cloud-free (<5%) and radiometrically stable conditions suitable for land use/land cover (LULC) analysis.

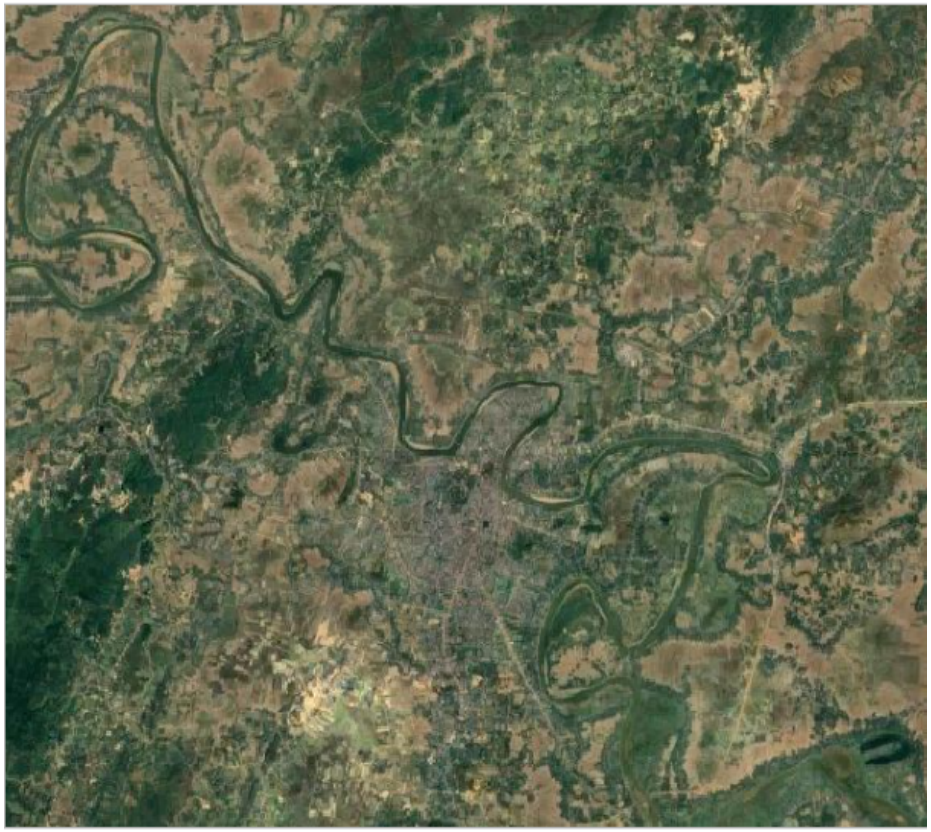

Fig. 1. Geographic extent of the study area Barak River basin

The area of study is shown in **figure 1**. The figure's resolution is 30 meters, and the QGIS software clips it to our desired area. It has four corners, the upper-left corner coordinate is 24.92051°N, 92.69716°E, upper-right corner coordinate is 24.91885°N, 92.89368°E and lower-right corner coordinate is 24.74158°N, 92.89336°E, lower-left corner coordinate is 24.74058°N, 92.69831°E this makes a 2D top-view picture of Barak River Basin. In the figure we can clearly see the most important city of Barak River Basin, Silchar and its surrounding rivers and vegetation areas.

4 Proposed Methodology

Recently, geospatial data has proven to be highly effective in producing detailed and comprehensible results for studying Land Cover and Land Use (LULC) across different regions. Like every technology, it comes with its advantages and limitations. One of the major challenges is the unavailability of labeled

datasets for specific areas. Using data from the Landsat 8 Operational Land Imager (OLI) [2], this work uses a multi-index method to address the absence of labeled datasets for the Barak River Basin. A multi-index approach enhances classification accuracy, reliability, and interpretability in remote sensing applications. It is an essential part of contemporary LULC mapping frameworks and is particularly important in areas with limited data, complex landscapes, or studies involving unsupervised techniques. The methodology encompasses satellite data preparation, spectral index computation for land cover categorization, unsupervised classification, and final validation through ground truthing. Spatial data has been classified into various categories and classes. In this study, we focus primarily on three classes and their complementary classes, as shown in **Table 2**, using different spectral indices. Otsu's thresholding [17] method is applied to the outcomes of each index to derive meaningful binary classifications. Each resulting binary image is then normalized to a common scale to allow comparison among indices and with the ground truth data.

Table 2. Name and description of diffrent LULC class scheme.

S.No.	Class Name	Description of Class
1	Vegetation	Forest, cropland, shrubland and grassland.
2	Non-Vegetation	Areas excluding vegetation-covered regions.
3	Water Bodies	Rivers, lakes, bays, and estuaries.
4	Non-Water Bodies	Areas excluding water bodies.
5	Built-up	Urban residential, commercial, industrial areas, vacant land, roads, transportation.
6	Non-Built-Up	Areas excluding built-up regions.

Figure 2 illustrates the complete methodology, detailing each step involved in the implementation of the proposed system. Landsat 8 imagery has 11 bands, for our proposed method required only 5 bands: band 2 for blue, band 3 for green, band 4 for red, band 5 for near-infrared (NIR), and band 6 for short-wave infrared (SWIR). Using those bands, indices are calculated for the specific classes. All index results have been evaluated to the Otsu threshold in order to get the binary-classified images. The kappa score for each index is obtained by comparing all of the binary imagery with the ground truth. The final unsupervised labelled data is generated using the most significant index in its class.

In the following subsections, we have discussed the data acquisition process, preprocessing techniques, and implementation of selected spectral indices to the acquired dataset. Furthermore, we provide a comprehensive overview of unsupervised classification methods and thresholding techniques on the outputs we got, and then we compare them to ground truth data to make sure they are correct.

Fig. 2. Methodology workflow for LULC classification using spectral indices

4.1 Satellite Data Acquisition and Preprocessing

Since 1972, NASA and USGS have worked together to develop the Landsat program, which offers reliable satellite imagery for LULC (land use and land

cover) analysis. Through the USGS Earth Explorer portal, surface reflectance data from Landsat 8, which is equipped with the Thermal Infrared Sensor (TIRS) and Operational Land Imager (OLI), were acquired for this study. The details of these bands are presented in **Table 2**. To ensure that vegetation, populated areas, and water bodies could be detected, imagery with less than 5% cloud cover and optimum seasonal conditions was chosen. To get the dataset ready for index computations, preprocessing techniques like band stacking, spatial clipping, and resampling were executed in QGIS. In the **Table 3**, first column is used for the types of sensors present in Landsat 8, second column for band number, column three for band name, column four shows the wavelength range taken by each band in micrometers (one millionth of a meter) and column five used for the resolution (in meters) for each band.

Table 3. Landsat 8 OLI and TIRS Band Specifications

S.No.	Instrument	Band	Band Name	Wavelength Range (µm)	Resolution (m)
1	OLI	Band 1	Coastal Aerosol	0.43 – 0.45	30
2	OLI	Band 2	Blue	0.45 – 0.51	30
3	OLI	Band 3	Green	0.53 – 0.59	30
4	OLI	Band 4	Red	0.64 – 0.67	30
5	OLI	Band 5	Near-Infrared (NIR)	0.85 – 0.88	30
6	OLI	Band 6	SWIR 1	1.57 – 1.65	30
7	OLI	Band 7	SWIR 2	2.11 – 2.29	30
8	OLI	Band 8	Panchromatic	0.50 – 0.68	15
9	OLI	Band 9	Cirrus	1.36 – 1.38	30
10	TIRS	Band 10	Thermal Infrared 1	10.6 – 11.19	100 (resampled to 30)
11	TIRS	Band 11	Thermal Infrared 2	11.50 – 12.51	100 (resampled to 30)

4.2 Spectral Index Computation

Every index is designed to indicate a particular surface characteristic using combinations of spectral reflectance bands. Vegetation, water bodies, and built-up areas are the most significant classes for Land Use and Land Cover (LULC) classification. The proposed methodology incorporates several spectral indices as discussed below.

4.2.1 Vegetation Indices : For Landsat 8 imagery, Bands 3 (Green), 4 (Red), and 5 (Near-Infrared, NIR) are used to compute vegetation indices including NDVI, MNDVI, GNDVI, and RVI:

– Normalized Difference Vegetation Index (NDVI), which is calculated as (NIR - RED) / (NIR + RED) where NIR is band 5 and RED is band 4.

- Modified Normalized Difference Vegetation Index (MNDVI), which is calculated as (NIR - RED) / SQRT(NIR + RED + 1) where NIR is band 5 and RED is band 4.
- Green Normalized Difference Vegetation Index (GNDVI), which is calculated as (NIR - GREEN) / (NIR + GREEN) where NIR is band 5 and GREEN is band 3.
- Ratio Vegetation Index (RVI), which is calculated as (NIR / RED) where NIR is band 5 and RED is band 4.

More positive values are more likely to indicate vegetation areas, while more negative or zero values resemble non-vegetation areas.

4.2.2 Water Indices : For detecting water bodies, Landsat 8 Bands 3 (Green), 4 (Red), 5 (NIR), and 6 (SWIR1) are employed to calculate NDWI, MNDWI, AWEI, and WRI:

- Normalized Difference Water Index (NDWI), which is calculated as (GREEN - NIR) / (GREEN + NIR) where NIR is band 5 and GREEN is band 3.
- Modified Normalized Difference Water Index (MNDWI), which is calculated as (GREEN - SWIR1) / (GREEN + SWIR1) where GREEN is band 3 and SWIR1 is band 6.
- Automated Water Extraction Index (AWEI), which is calculated as $4 \times$ (GREEN - SWIR1) - $(0.25 \times$ NIR + $2.75 \times$ SWIR1) where NIR is band 5, GREEN is band 3, and SWIR1 is band 6.
- Water Ratio Index (WRI), which is calculated as (GREEN + RED) / (NIR + SWIR1) where NIR is band 5, RED is band 4, GREEN is band 3, and SWIR1 is band 6.

More positive values are more likely to indicate water bodies, while more negative or zero values resemble non-water bodies.

4.2.3 Built-up Indices : To identify built-up regions, indices such as NDBI, UI, and BI are calculated using Bands 2 (Blue), 3 (Green), 4 (Red), 5 (NIR), and 6 (SWIR1):

- Normalized Difference Built-up Index (NDBI), which is calculated as (SWIR1 - NIR) / (SWIR1 + NIR) where NIR is band 5 and SWIR1 is band 6.
- Urban Index (UI), which is calculated as (SWIR1 - BLUE) / (SWIR1 + BLUE) where BLUE is band 2 and SWIR1 is band 6.
- Built-up Index (BI), which is calculated as BI = Normalized Difference Built-up Index (NDBI) - Normalized Difference Vegetation Index (NDVI).

More positive BI values generally indicate built-up surfaces, while negative or zero values suggest non-urban features.

4.3 Unsupervised Classification and Thresholding

In this section, we discuss the techniques of unsupervised classification, thresholding, and clustering. To transform spectral index information into meaningful land cover classes, a structured multi-step classification methodology was adopted.

4.3.1 Index Normalization : All spectral indices are normalized to a common scale between 0.0 and 1.0 to enable reliable and meaningful comparisons between different spectral indices. This step is very crucial to avoid the bias included by differing value ranges. For normalization we performed min-max scaling [13] , where each pixel value was transformed using the equation:

$$\text{Normalized Value} = \frac{X - X_{\min}}{X_{\max} - X_{\min}} \tag{1}$$

where

- X represents the original index value,
- $X_{\min}$ denotes the minimum value of that index within the dataset,
- $X_{\max}$ denotes the maximum value of that index within the dataset.

4.3.2 Otsu's Thresholding : Otsu's method [17] was applied to each normalized index layer to compute optimal threshold values. This algorithm maximizes the inter-class variance and minimizes the intra-class variance, resulting in an effective binary classification. It enables separation of classes such as:

- Vegetation vs. Non-vegetation,
- Water vs. Non-water,
- Built-up vs. Non built-up.

The step by step process to compute otsu thresholding is discussed in the **algorithm 1**.

4.3.3 Clustering and Masking Every pixel of the data was evaluated using the normalized indices of built-up, water, and vegetation and allocated to the class with the highest index value. The masking operation is applied to segregate every land cover class. Binary masks were generated for each class using Otsu's thresholding. Utilizing the unsupervised classification approach, the comparative index-based clustering finally classified the pixels into vegetation, water bodies, and built-up areas without the need for any pre-labeled training data.

4.4 Ground Truthing

The ground truth data is gathered by physically reaching the ground truth points and capturing the images of that point with its coordinates. The steps of generating the ground truth are discussed below.

Algorithm 1 Otsu's Thresholding Algorithm

Input: Grayscale image with L gray levels $[1, 2, \ldots, L]$
Output: Optimal threshold k^*
Compute histogram of the image
Normalize histogram: $p_i = \frac{n_i}{N}$, where n_i is the number of pixels at level i and N is total pixels
Initialize: $\omega(k) \leftarrow 0$, $\mu(k) \leftarrow 0$, $\mu_T \leftarrow \sum_{i=1}^{L} i \cdot p_i$, $\sigma^2_{\max} \leftarrow 0$, $k^* \leftarrow 0$
for $k = 1$ to $L - 1$ **do**
    Compute $\omega(k) = \sum_{i=1}^{k} p_i$
    Compute $\mu(k) = \sum_{i=1}^{k} i \cdot p_i$
    if $\omega(k) = 0$ or $\omega(k) = 1$ **then**
        continue
    end if
    Compute between-class variance:

$$\sigma_b^2(k) = \frac{[\mu_T \cdot \omega(k) - \mu(k)]^2}{\omega(k) \cdot (1 - \omega(k))}$$

    if $\sigma_b^2(k) > \sigma^2_{\max}$ **then**
        $\sigma^2_{\max} \leftarrow \sigma_b^2(k)$
        $k^* \leftarrow k$
    end if
end for
return k^*

- For capturing the image with coordinates, we used GPS Map Camera Application for 102 random points within the study area.
- The data must be documented and stored in structured `.csv` format to import in QGIS software for generating the georeferenced ground truth in `.tiff` format.

In **figure 3** we showed the collected data, with samples of the vegetation class (a) and (f), the built-up class (b) and (e), and finally the water class (c) and (d) with the coordinates.

5 Result and Validation

In this section we have discussed results and compared the outputs with ground truth. The selected sample points are compared with classified results to achieve accuracy. Accuracy metrics such as kappa Coefficient were calculated to evaluate the performance of the classification.

5.1 Classification Result Comparisons

Visual comparisons between the classified results and the ground truth are carried out across three major land cover categories:

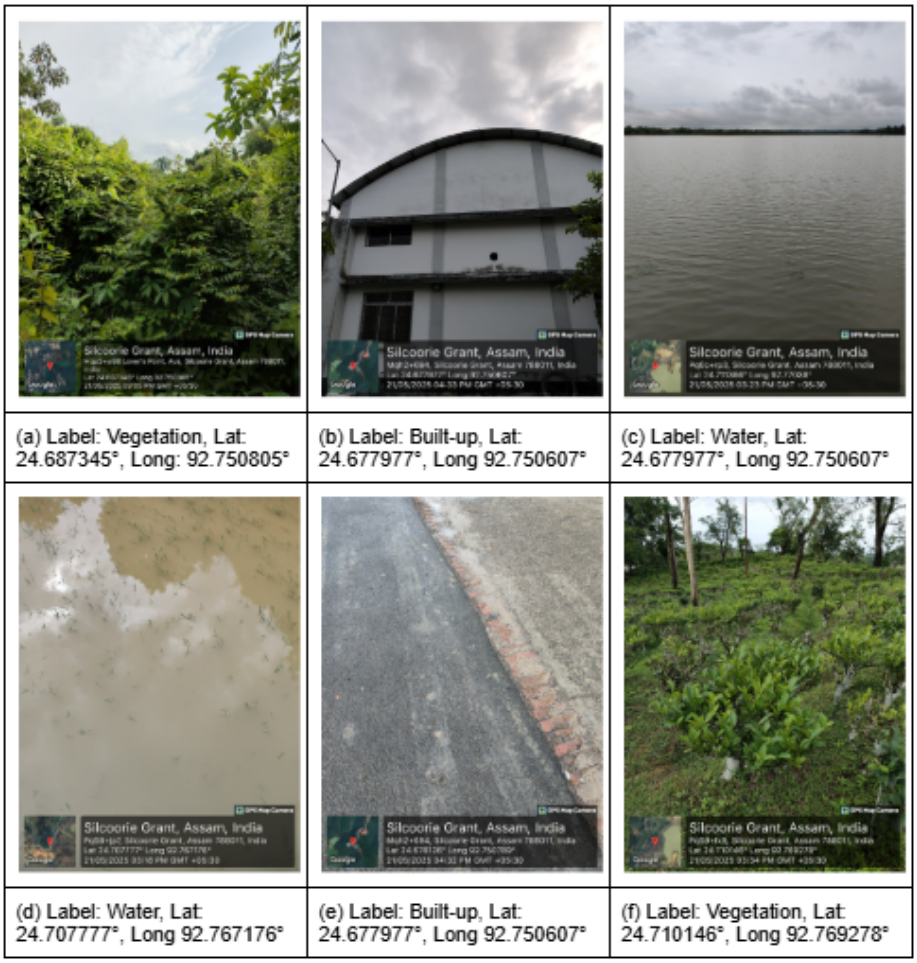

Fig. 3. sample of ground truth

5.1.1 Vegetation Classification Comparison : In **figure 4**, the green color refers to the vegetation areas and the red color area refers to the non-vegetation areas. Those are the binary classified images after applying otsu's thresholding. NDVI (a) and MNDVI (b) show very similar and almost accurate results. GNDVI (c) produces inaccurate results with marking non-vegetation areas as vegetation. RVI (d) produces average and noisy results

5.1.2 Water Body Classification Comparison : In **figure 5**, the blue color refers to the water bodies and the white color area refers to the non-water bodies. Those are the binary classified images after applying otsu's thresholding.

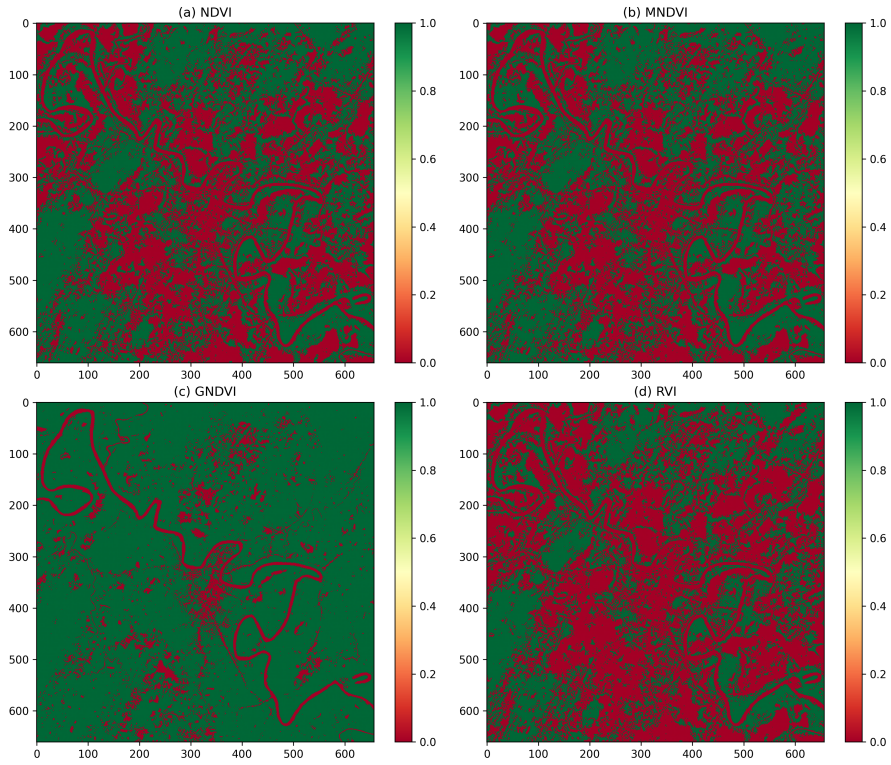

Fig. 4. (a) NDVI, (b) MNDVI, (c) GNDVI and (d) RVI indices output (vegetation).

WRI (d) gives the best output among others. NDWI (a) and MNDWI (b) show similar and almost accurate results. AWEI (c) produces inaccurate results with marking non-water bodies as water bodies.

5.1.3 Built-up Area Classification Comparison : In **figure 6**, the black color refers to the built-up area and the white color area refers to the non-built-up bodies Those are the binary classified images after applying otsu's thresholding. BI (c) gives the best output among others. NDBI (a) show similar and almost accurate results. UI (c) produces inaccurate results with marking non-built-up areas as built-up areas.

5.2 Kappa Coefficient (κ)

The Kappa coefficient is a statistical metric that measures the agreement between the observed (ground truth) and predicted classifications, adjusted for

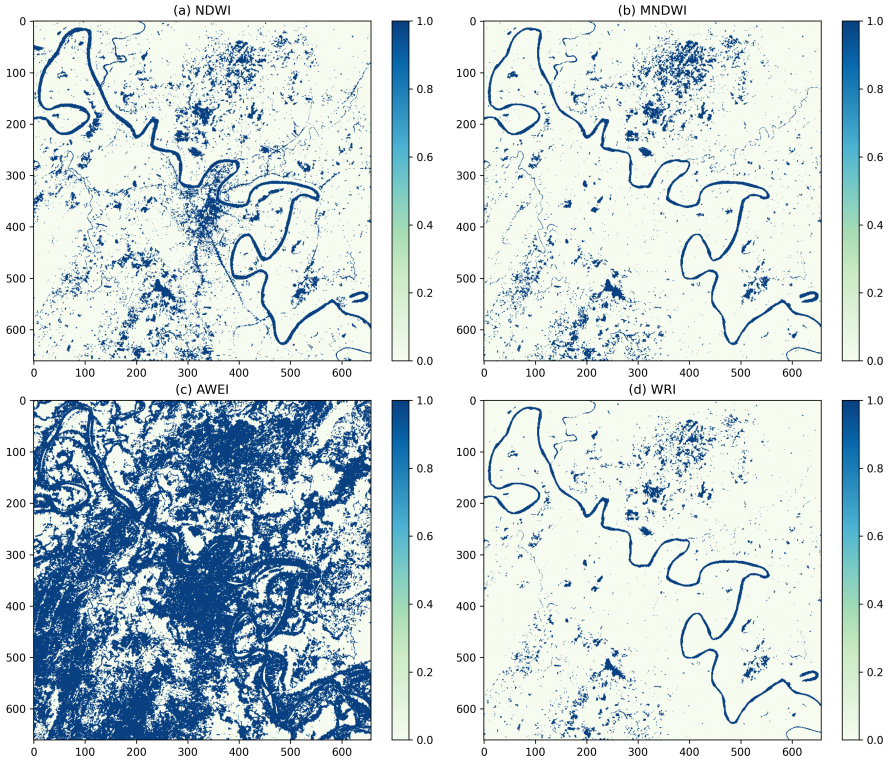

Fig. 5. (a) NDWI, (b) MNDWI, (c) AWEI and (d) WRI indices output (Water Bodies).

chance agreement. It is calculated as:

$$\kappa = \frac{p_o - p_e}{1 - p_e} \tag{2}$$

Where:

- p_o = observed agreement
- p_e = expected agreement by chance

In **table 4** , Kappa values (κ) are shown, the range and its significance level. More the value close to +1 more it is close to almost perfect agreement and 0 or less than zero says no agreement. The comparative result of all indices with Ground Truth(GT) is shown with the kappa score and the final rank of each category in **table 5**. For vegetation classification, the NDVI performed the best with 0.93 Kappa score, showing a very strong match with ground truth. NDVI achieved the highest score for vegetation due to its proven sensitivity to chlorophyll content and dense vegetation. MNDVI and RVI performed well, but GNDVI showed

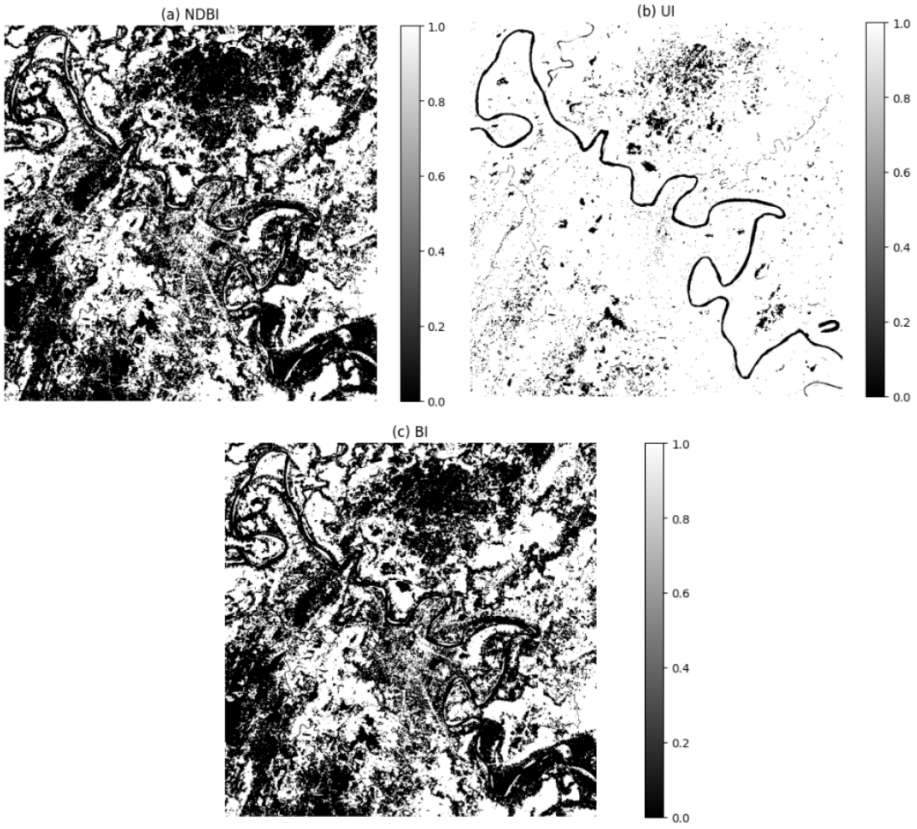

Fig. 6. (a) NDBI,(b) UI, and (c) BI indices output (Built-up Area).

Table 4. Interpretation of Kappa Coefficient Values

S.No.	Kappa Value (κ)	Level of Agreement
1	< 0	No agreement
2	0.01 – 0.20	Slight agreement
3	0.21 – 0.40	Fair agreement
4	0.41 – 0.60	Moderate agreement
5	0.61 – 0.80	Substantial agreement
6	0.81 – 1.00	Almost perfect agreement

poor results for this Barak River Basin area.MNDVI is designed to reduce atmospheric and background noise, which may have reduced contrast in dense tropical vegetation such as those found in the Barak River Basin and it affects the result

of MNDVI. RVI commonly performed well for open, dry vegetation zones, it is sensitive to illumination variations and soil background, which are common in the Barak Basin due to its hilly terrain and heterogeneous soil which can cause saturated results. GNDVI is very sensitive to chlorophyll content but less effective in mixed vegetation-soil backgrounds which may cause poor results in the Barak River Basin. For identifying water bodies, the WRI achieved the highest Kappa score (0.83), making it the most suitable among other tested water indices.WRI effectively enhances the spectral response of water features while suppressing the signal from vegetation and soil with best results in the Barak River Basin area. MNDWI and NDWI offered moderate accuracy, but AWEI performed very poorly for this Barak River Basin area.MNDWI uses a SWIR band which can also reflect from exposed soil, wet soil and sandbanks, reducing water detection accuracy. NDWI performs well in open water detection, but in the Barak Basin, sediment-laden water and mixed water-vegetation pixels lead to misclassification and reduce its efficacy. AWEI is designed to remove shadows effectively in urban scenes or cloud-shadow environments, but we use less than 5% cloudy data and confuse water with dark shadows from dense forest or steep slopes, leading to poor detection. For built-up area detection, the Built-up Index (BI) scored highest (0.81), and NDBI shows average performance.BI achieved the best results among built-up indices because it captures the contrast between built-up surfaces and their surroundings, especially in urban-rural transition zones like the Barak River Basin. The Urban Index (UI) showed weak agreement for this Barak River Basin area. NDBI uses the difference between SWIR and NIR bands. It can confuse bare soil and dry riverbeds with urban structures, which are common in the Barak Basin. The Urban Index is optimized for high-density urban zones, which are rare in the Barak River Basin, resulting in a very low Kappa score.

Table 5. Kappa Scores and Ranks for Indices by Category

Category	Index vs Ground Truth	Kappa Score	Rank
Vegetation	NDVI vs GT	**0.9324**	1st
	MNDVI vs GT	0.8201	2nd
	RVI vs GT	0.8164	3rd
	GNDVI vs GT	0.2844	4th
Water Body	WRI vs GT	**0.8283**	1st
	MNDWI vs GT	0.6329	2nd
	NDWI vs GT	0.6065	3rd
	AWEI vs GT	0.1409	4th
Built-up	BI vs GT	**0.8144**	1st
	NDBI vs GT	0.7780	2nd
	UI vs GT	0.1327	3rd

5.3 Unsupervised Classified Result

In our study NDVI, WRI, and BI proved to be the most effective indices in their respective categories. Utilizing those indices we are able to generate the final unsupervised label data shown in Figure 7. Where the red color shows the built-up area, blue color resembles all types of water bodies, green shows the vegetation area and lastly black incorporates the background.In conclusion, by implementing NDVI, WRI and BI we are able to label the data using this unsupervised proposed methodology.

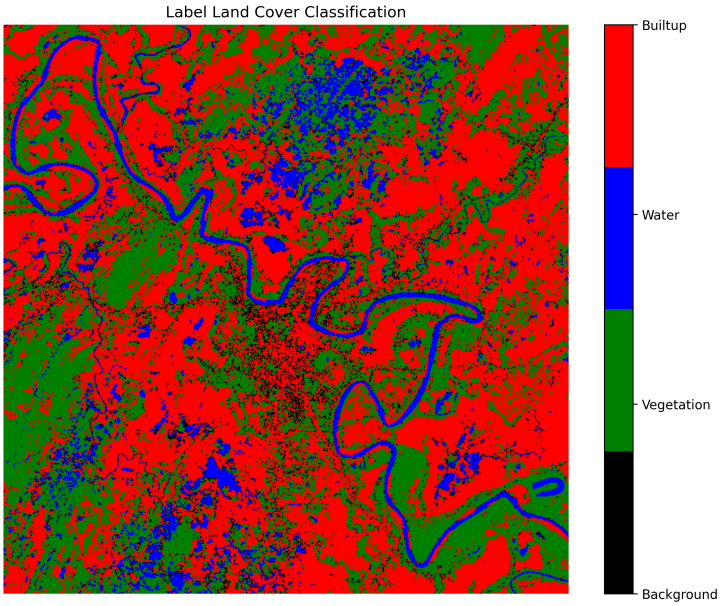

Fig. 7. Visualization of NDBI, UI, and BI indices.

6 Conclusion and Future Scope

The supervised classification plays a crucial role in remote sensing data analysis, but to achieve this requires a sufficient amount of label data set. The Barak River Basin area is lacking on that label data set so it is important to improvise unsupervised methods for this region.The proposed methodology successfully

overcomes the problem for Barak River Basin. This study shows, among multiple spectral indices applied, the NDVI proved to be the most effective for vegetation classification, the WRI performed best among other indices in detecting water bodies, and the BI worked accurately to evaluate built-up areas. Utilizing these top-performing indices, we successfully generated an unsupervised LULC classification for the Barak River Basin despite the limitation of having no labeled datasets.

In future, this methodology can be used for the development of a large-scale, temporally rich LULC dataset for the Barak River Basin. That dataset could be used for spatiotemporal change analysis, supporting environmental monitoring, urban expansion studies, flood risk assessment, and land management planning in the region. With further integration of high-resolution satellite data and limited ground truthing, this technique can evolve into a scalable, semi-automated pipeline for long-term geospatial monitoring across similar underrepresented and ecologically sensitive regions.

Acknowledgement

This work was supported by the sponsored project under the **Department of Science and Technology (DST), Govt. of India - Tribal Sub-Plan (TSP)** scheme of IIT Bhilai Innovation and Technology Foundation (IBITF), **Sanction Number:** IBITF/Note/TSP/SanctionLetter/2024-25/0125.

References

1. L. Bencherif, H. Bougherara, and R. Boudjemaa. Mapping typical lulc classes using spatiotemporal analysis and the thresholds of spectral optical satellite imagery indices: a case study in algiers city. *Environmental Monitoring and Assessment*, 195(11):1351, 2023.
2. S. Bouzekri, H. Wu, and A. Shamsoddini. A new spectral index for the detection of built-up areas: Development and application to the landsat-8 imagery. *Journal of the Indian Society of Remote Sensing*, 43:867–875, 2015.
3. C. Chandramouli. *Census of India 2011: Provisional Population Totals*. Registrar General & Census Commissioner, New Delhi, 2011.
4. Russell G. Congalton. A review of assessing the accuracy of classifications of remotely sensed data. *Remote Sensing of Environment*, 37(1):35–46, 1991.
5. S. Dutta. Urbanization in barak valley: A geographical analysis. *North Eastern Geographer*, 34(1-2):45–52, 2002.
6. S. Dutta and B. Roy. Development trends in barak valley. *Geographical Review of India*, 68(3):211–218, 2006.
7. Peng Gong, Jianya Wang, Le Yu, Yong Zhao, Yao Zhao, Lu Liang, Zheng Niu, Xin Huang, Haizeng Fu, and Shaoqing Liu. Global land cover mapping at 30 m resolution: A pok-based operational approach. *ISPRS Journal of Photogrammetry and Remote Sensing*, 103:7–27, 2020.
8. M. S. Hossain, M. Rahman, and S. Akter. Land use and land cover change detection using ndvi and savi in fashiakhali wildlife sanctuary, bangladesh. *Environmental Challenges*, 10:100752, 2023.

9. A. R. Huete. A soil-adjusted vegetation index (SAVI). *Remote Sensing of Environment*, 25(3):295–309, 1988.
10. John R. Jensen. *Introductory Digital Image Processing: A Remote Sensing Perspective*. Prentice Hall, 3rd edition, 2005.
11. R. Kaur and A. C. Pandey. A review of remote sensing indices for built-up area extraction with a focus on urban planning and sustainability. *Arabian Journal of Geosciences*, 15:1199, 2022.
12. Rajveer Kaur and Puneeta Pandey. A review on spectral indices for built-up area extraction using remote sensing technology. *Arabian Journal of Geosciences*, 15:1–14, 2022.
13. Xiaoyong Liu, Xiaohui Yuan, and H Felix Lee. A robust data scaling algorithm to improve classification accuracies in biomedical data. *BMC Bioinformatics*, 17(1):1–13, 2016.
14. D. Lu and Q. Weng. A survey of image classification methods and techniques for improving classification performance. *International Journal of Remote Sensing*, 28(5):823–870, 2007.
15. S. K. McFeeters. The use of the normalized difference water index (ndwi) in the delineation of open water features. *International Journal of Remote Sensing*, 17(7):1425–1432, 1996.
16. Salem Morsy and Mashaan Hadi. Impact of land use/land cover on land surface temperature and its relationship with spectral indices in dakahlia governorate, egypt. *International Journal of Engineering and Geosciences*, 7(3):272–282, 2022.
17. Nobuyuki Otsu. A threshold selection method from gray-level histograms. *IEEE Transactions on Systems, Man, and Cybernetics*, 9(1):62–66, 1979.
18. J. Pattanayak and P. G. Diwakar. Seasonal variability analysis using ndvi, ndwi and ndbi in hyderabad region. In *2018 IEEE International Geoscience and Remote Sensing Symposium (IGARSS)*, pages 1280–1283. IEEE, 2018.
19. Surya Prakash Pattanayak and Sumant Kumar Diwakar. Seasonal comparative study of ndvi, ndbi and ndwi of hyderabad city (telangana) based on liss-iii image using remote sensing and dip. *Khoj: An International Peer Reviewed Journal of Geography*, 5:78–86, 2018.
20. M. A. Rahman, B. Das, and M. N. Ahmed. Land use and land cover dynamics and their impacts on ecosystem services in the barak river basin. *Ecological Indicators*, 125:107557, 2021.
21. David P. Roy, Michael A. Wulder, Thomas R. Loveland, Curtis E. Woodcock, Robert G. Allen, Martha C. Anderson, Dennis Helder, James R. Irons, David M. Johnson, Robert Kennedy, Ted A. Scambos, Crystal B. Schaaf, John R. Schott, Yang Sheng, Eric F. Vermote, and Alan S. Belward. Landsat-8: Science and product vision for terrestrial global change research. *Remote Sensing of Environment*, 145:154–172, 2014.
22. M. Roy and M. P. Bezbaruah. Agricultural development in the barak valley region. *Indian Journal of Regional Science*, 34(1):55–62, 2002.
23. H. S. Sharma. *Physiography of the North East India*. National Book Trust, New Delhi, 1970.
24. H. S. Sharma. *Urban Development in North East India*. Mittal Publications, New Delhi, 2003.
25. A. Singh, R. Setia, and P. Sharma. Comparative analysis of water indices to detect surface water bodies in satellite images. *Journal of the Indian Society of Remote Sensing*, 43(3):625–635, 2015.

26. X. Sun, X. Li, B. Tan, J. Gao, L. Wang, and S. Xiong. Integrating otsu thresholding and random forest for land use/land cover (lulc) classification and seasonal analysis of water and snow/ice. *Remote Sensing*, 17(5):797, 2025.
27. E. Suryani, E. I. Asmari, and B. Harjito. Image segmentation of acute myeloid leukemia using multi otsu thresholding. *Journal of Physics: Conference Series*, 1803:012016, 2021.
28. Nazimur Rahman Talukdar, Biswajit Singh, and Parthankar Choudhury. Conservation status of some endangered mammals in barak valley, northeast india. *Journal of Asia-Pacific Biodiversity*, 11:167–172, 2018.
29. Compton J. Tucker. Red and photographic infrared linear combinations for monitoring vegetation. *Remote Sensing of Environment*, 8(2):127–150, 1979.
30. U.S. Geological Survey. Earthexplorer, n.d. Accessed: 2025-05-08.
31. Y. Xie, Z. Sha, and M. Yu. Remote sensing imagery in vegetation mapping: a review. *Journal of Plant Ecology*, 1(1):9–23, 2008.
32. H. Xu. Modification of normalized difference water index (ndwi) to enhance open water features in remotely sensed imagery. *International Journal of Remote Sensing*, 27(14):3025–3033, 2006.
33. Muhammad Yazrin Yasin, Jamalunlaili Abdullah, Norzailawati Mohd Noor, Mariney Mohd Yusoff, and Nisfariza Mohd Noor. Landsat observation of urban growth and land use change using ndvi and ndbi analysis. *IOP Conference Series: Earth and Environmental Science*, 540(1):012070, 2020.
34. Y. Zha, J. Gao, and S. Ni. Use of normalized difference built-up index in automatically mapping urban areas from tm imagery. *International Journal of Remote Sensing*, 24(3):583–594, 2003.